



Cite this: *Chem. Commun.*, 2017, 53, 451

Received 30th September 2016,
Accepted 7th December 2016

DOI: 10.1039/c6cc07927j

www.rsc.org/chemcomm

Developing high-performance small molecule organic solar cells *via* a large planar structure and an electron-withdrawing central unit†

Hongtao Zhang,^{ab} Yongtao Liu,^a Yanna Sun,^{ab} Miaomiao Li,^a Bin Kan,^a Xin Ke,^{ab} Qian Zhang,^a Xiangjian Wan^{ab} and Yongsheng Chen^{*ab}

We designed and synthesized a new small molecule donor material named DR3TBDD using an electron-withdrawing unit BDD as the central building block. A PCE of 9.53% with a high V_{oc} of around 1 V was achieved.

Bulk heterojunction (BHJ) organic photovoltaics (OPVs), with the advantages of being solution processable, light weight, low cost and flexible, are promising sustainable solar energy converters as an alternative solution to increasing energy problems all over the world.^{1,2} In recent years, significant effort has been made on both polymer and small molecule based bulk heterojunction (BHJ) OPVs and impressive power conversion efficiencies (PCEs) have been achieved.^{3–11} As compared to polymer based OPVs (P-OPVs), small molecule based OPVs (SM-OPVs) have several distinct advantages including well-defined chemical structures, less batch-to-batch variation and generally higher open-circuit voltages (V_{oc}).^{12–20} Based on the equation $PCE = V_{oc} \times J_{sc} \times FF/P_{in}$, PCEs depend on three parameters (V_{oc} , J_{sc} , and FF). In most previous works for SM-OPVs, it is hard to improve V_{oc} , which is highly correlated with the energy level difference between the highest occupied molecular orbital (HOMO) of the donor and the lowest unoccupied molecular orbital (LUMO) of the acceptor, while maintaining both high J_{sc} and FF simultaneously for bulk heterojunction OPVs.²¹ Thus, further increasing V_{oc} of SM-OPVs while keeping high FF and J_{sc} is an important strategy to obtain an outstanding PCE.

In recent years, our group have reported a series of small molecules with the A–D–A structure, and it is found that small molecules with deep HOMO energy levels could generate an

increased V_{oc} , in which the deep HOMO energy level was tuned by using weak electron-donating units such as fluorene and carbazole as core units in these A–D–A type small molecules. However, the photovoltaic performance of devices based on these molecules exhibited low PCEs of around 2–4%, attributed to the low FF and J_{sc} values led by the unfavorable active layer morphologies. Besides the device optimization strategies such as thermal annealing, additive, *etc.*, the intrinsic properties of the active layer molecules such as the packing mode, miscibility, *etc.* also play a major role. Therefore, great effort has been made to design new donor and acceptor materials in the OPV community. On the one hand, using electron-withdrawing units in D–A polymers has been demonstrated as an effective strategy to lower the HOMO level.²² Thus, it is worth trying electron-withdrawing groups on the central core to tune the HOMO energy level of small molecules. On the other hand, previous works indicated that planar structure units could improve the FF and J_{sc} values of OPV devices,²³ so it is desirable to use planar structure units as the core in A–D–A type small molecules to maintain the high FF and J_{sc} . Along these lines, herein, we designed and synthesized a small molecule named DR3TBDD, using a unit named 1,3-bis(4-(2-ethylhexyl)thiophen-2-yl)-5,7-bis(2-ethylhexyl)benzo[1,2-*c*:4,5-*c'*]-dithiophene-4,8-dione (BDD) with strong electron-withdrawing ability and a large planar structure as the central core.^{24–26} The photovoltaic performance as well as other properties of DR3TBDD were studied. The HOMO energy level is -5.12 eV, which is deeper than most of high photovoltaic performance small molecules. For small molecule donors, it is indeed widely observed that their V_{oc} is higher than polymer donors with the same acceptor.^{27,28} Thus, a higher V_{oc} value is expected for the devices using DR3TBDD as the donor compared with those in which polymer donors are used.

Optimal OPV devices based on DR3TBDD: PC₇₁BM as the active layer exhibited a PCE of 9.53%, with a V_{oc} of 0.97 V, a J_{sc} of 14.77 mA cm⁻², and a FF of 66.9%. Note, indeed, that this V_{oc} value is one of the highest values among high performance SM-OPVs, significantly higher than most of the polymer donor

^a The Centre of Nanoscale Science and Technology and Key Laboratory of Functional Polymer Materials, State Key Laboratory and Institute of Elemento-Organic Chemistry, Collaborative Innovation Center of Chemical Science and Engineering (Tianjin), College of Chemistry, Nankai University, Tianjin, 300071, China. E-mail: yschen99@nankai.edu.cn

^b School of Materials Science and Engineering, National Institute for Advanced Materials, Nankai University, Tianjin 300071, China

† Electronic supplementary information (ESI) available: Details of the synthesis and characterization of DR3TBDD, TGA, and CV. See DOI: 10.1039/c6cc07927j

based devices. Meanwhile, J_{sc} and FF of DR3TBDD based SM-OPVs remain very high too, resulting in the excellent PCE of 9.53%.

The detailed synthetic procedures and characterization data of DR3TBDD are presented in the ESI.† The molecule showed good solubility in common organic solvents, such as chloroform, chlorobenzene, *etc.* Thermogravimetric analysis (Fig. S2, ESI†) indicated below 5% mass loss at 390 °C under a N₂ atmosphere.

Theoretical calculations were performed by using the density functional theory (DFT). To simplify the calculations, alkyl chains were replaced by methyl groups. As shown in Fig. S4 (ESI†), the HOMO of the small molecule is delocalized on thiophenes and BDD units and the LUMO of the small molecule is localized on thiophenes and the end groups, which indicates that the HOMO energy level of the small molecule was mainly tuned by the central electron-withdrawing units. This result demonstrates that using electron-withdrawing units as central units is indeed an efficient way to tune the HOMO energy level of small molecules. Meanwhile, the geometry optimizations yielded nearly planar structures for the small molecule, as shown in Fig. 1c, which is favorable for π - π stacking between the molecule backbones. The UV-vis absorption spectra of DR3TBDD are shown in Fig. 1b. The absorption of DR3TBDD in a diluted CHCl₃ solution shows a peak at 510 nm. In a solid film, the spectrum is broadened and red-shifted with two comparable maximum absorptions at 605 and 654 nm, indicating the effective π - π stacking between the molecule backbones and it may be

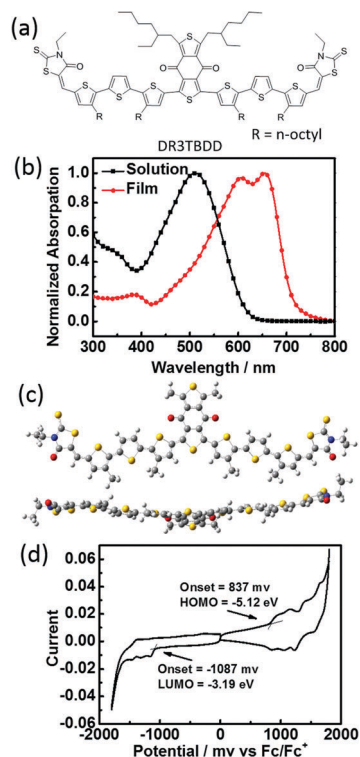


Fig. 1 (a) The chemical structure of DR3TBDD; (b) UV-vis absorption spectra of DR3TBDD in chloroform solution and as-cast film. (c) Optimized molecular geometries (side view and top view) of DR3TBDD using DFT. (d) The electrochemical cyclic voltammetry curve of DR3TBDD.

beneficial for charge transport.^{29–31} The optical band gap estimated from the onset of the film absorption is 1.68 eV. In investigating the electrochemical properties of DR3TBDD, cyclic voltammetry was used to determine the energy levels. The potentials were internally calibrated using ferrocene/ferrocenium of the redox couple (4.80 eV below the vacuum level). The CV curves are displayed in Fig. S3 (ESI†). The HOMO and LUMO energy levels were -5.12 and -3.19 eV, respectively, which were calculated from the onset oxidation potential and reduction potential, respectively. The electrochemical band gap of DR3TBDD was estimated to be about 1.93 eV. The above data suggest that DR3TBDD would be a good donor material for OPVs with the widely used acceptor PCBM.

Solution-processed bulk heterojunction solar cells using DR3TBDD as the electron donor material with a device structure of glass/ITO/PEDOT:PSS/DR3TBDD:PC₇₁BM/PrC60MA /Al were fabricated. PrC60MA is a methanol-soluble fullerene-surfactant developed by Alex K.-Y as an efficient interfacial layer for cathodes,³² and its structure is shown in Fig. S5 (ESI†). Typical current density–voltage (J - V) curves of solar cells with different post-treatments are presented in Fig. 2, and the corresponding device parameters are summarized in Table 1. With a series of testing, the optimal donor/acceptor weight ratio was obtained to be 1:0.8, and the device without any treatment shows a moderate PCE of 3.21%, with a V_{oc} of 1.02 V, a J_{sc} of 8.35 mA cm^{-2} , and a FF of 37.6%. After thermal annealing (TA) at 100 °C for 10 min, the PCE increased to 5.74%, with a V_{oc} of 1.04 V, a J_{sc} of 10.52 mA cm^{-2} , and a FF of 52.3%. As an effective approach, solvent vapor annealing (SVA) has been used in polymer based OSC devices to fine-tune the morphology of the active layer.³³ Thus, this approach was employed in the following device optimization. With chloroform vapor annealing for 60 s, the PCE

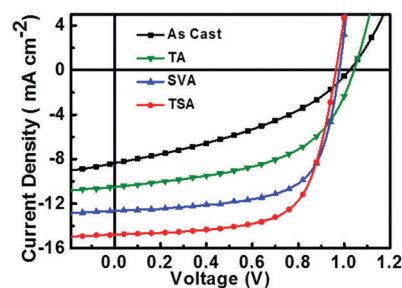


Fig. 2 J - V curves of BHJ devices prepared from DR3TBDD blend with PC₇₁BM of DR3TBDD:PC₇₁BM blend films with different treatments.

Table 1 Device performance for BHJ solar cells based on DR3TBDD:PC₇₁BM

Treatment	V_{oc} (V)	J_{sc} (mA cm^{-2})	FF	PCE ^{a,b} (%)
None	1.02 ± 0.01	8.02 ± 0.30	0.36 ± 0.01	2.90 ± 0.31 (3.21)
TA	1.03 ± 0.01	10.49 ± 0.25	0.51 ± 0.02	5.48 ± 0.26 (5.74)
SVA	0.97 ± 0.01	12.48 ± 0.17	0.64 ± 0.02	7.78 ± 0.38 (8.16)
TSA	0.96 ± 0.01	14.59 ± 0.18	0.66 ± 0.01	9.23 ± 0.30 (9.53)

^a The average values are obtained from 30 devices. ^b The best PCEs are provided in parentheses.

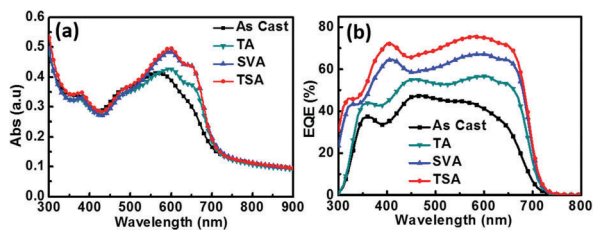


Fig. 3 (a) UV-vis absorption spectra of the DR3TBDD:PC₇₁BM blend film with different treatments and (b) EQE curves of DR3TBDD based devices with different treatments.

improved to 8.16%, with a V_{oc} of 0.98 V, a J_{sc} of 12.65 mA cm⁻², and a FF of 65.8%. In combination with TA, the active layer was exposed to chloroform vapor for 60 s after TA. Surprisingly, the PCE sharply improved to 9.53% with the thermal-solvent annealing (TSA), with a V_{oc} of 0.97 V, a J_{sc} of 14.77 mA cm⁻², and a FF of 66.9%. This excellent PCE was attributed to the simultaneously high V_{oc} , J_{sc} and FF values. Herein, the high V_{oc} value was attributed to the deep HOMO energy level of DR3TBDD, which was consistent with our expectation and the high J_{sc} as well as FF was originated from the outstanding absorption properties, preferably morphology, and the higher and more balanced charge mobilities as discussed below. In order to study the effect of thermal annealing and solvent vapor annealing on the photovoltaic performance, UV-vis absorption spectra of blend films of DR3TBDD and PC₇₁BM were recorded. Fig. 3a shows the absorption spectra of the blend films. Compared to the absorption spectra of the as-cast blend film, the maximum absorption peaks of the blend films shifted from 575 to 608, 605 and 606 nm with thermal annealing, solvent vapor annealing and both of thermal and solvent annealing, respectively. The optimized blend films showed shoulder peaks at 651, 646 and 636 nm, which indicates the enhancement of π - π stacking between the molecule backbones, thus resulting in improved J_{sc} . External quantum efficiency (EQE) is the ratio of the number of collected charge carriers to the number of incident photons of the solar cell, and has been widely used to characterize the light response for different wavelengths and efficiencies. These results are shown in Fig. 3b. For the devices with thermal annealing, solvent annealing and both of thermal and solvent annealing, uniform increases of the light response across the wavelength range of 300–730 nm are all observed in comparison with that of the as-cast device. It is worth noting that a maximum value of 75.6% was obtained for the device when both of thermal and solvent annealing was applied. The calculated J_{sc} values obtained from the EQE curves are 7.09, 10.47, 12.58, and 14.07 mA cm⁻², respectively, for the four different treatments. All the calculated J_{sc} values show less than 5% mismatch compared with the J_{sc} values obtained from the J - V curves.

To gain insight into the surface morphology of the blend films of DR3TBDD:PC₇₁BM, atomic force microscopy (AFM) was used. As shown in Fig. 4, without any treatment, the blend film shows a root-mean-square (RMS) roughness of 0.55 nm. After thermal annealing, solvent annealing and both thermal annealing and solvent annealing, the RMS value changes to 1.17, 0.63, 1.33 nm, respectively. Transmission electron microscopy (TEM) was also

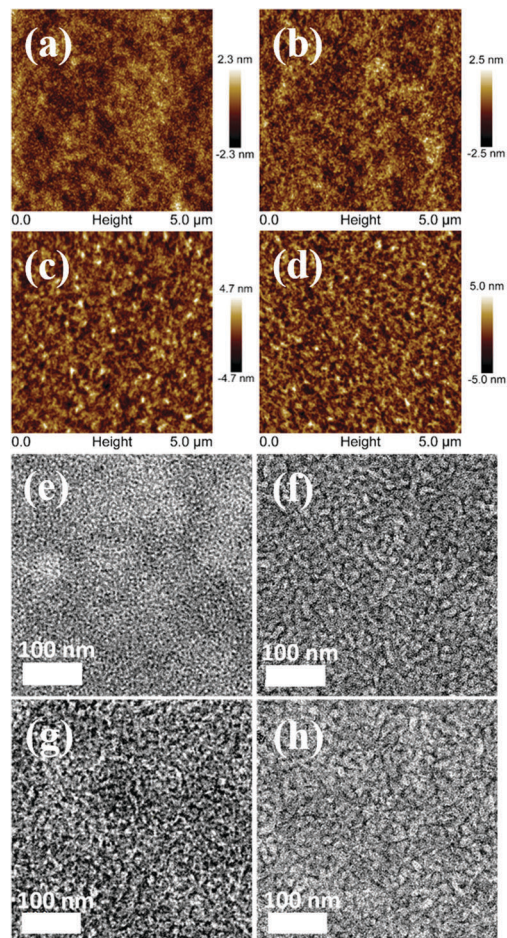


Fig. 4 (a–d) AFM images and (e–h) TEM images of the active layer based on DR3TBDD:PC₇₁BM, (a and e) as-cast; (b and f) with thermal annealing; (c and g) with solvent annealing; and (d and h) with both thermal and solvent annealing. The scale bar of TEM images is 100 nm.

used to investigate the morphology of the active layer, shown in Fig. 4. Compared with the as-cast film, a better phase separation was observed after thermal annealing and solvent annealing. With both thermal and solvent annealing, a clear fibrillar morphology with a bicontinuous interpenetrating network was observed. Note that the fibril width with the TSA is larger than that with the SVA and smaller than that with the TA. The fibrils with the TSA treatment are more favorable for exciton diffusion/dissociation and charge transport. These would also be beneficial to high J_{sc} and FF.

The hole mobilities and electron mobilities of the as-cast blend films and optimized blend films were measured using the space-charge-limited-current (SCLC) method (Fig. 5). For the as-cast blend films, the hole mobilities and electron mobilities were 3.21×10^{-5} and 7.17×10^{-5} cm² V⁻¹ s⁻¹, respectively. After both thermal and solvent vapor annealing, higher and more balanced hole mobilities and electron mobilities of 1.08×10^{-4} and 7.06×10^{-5} cm² V⁻¹ s⁻¹ were obtained, respectively, which are beneficial for higher FF and J_{sc} , consistent with the results of FF and J_{sc} obtained from J - V curves.

In conclusion, a new small molecule donor material named DR3TBDD using BDD with a planar structure and strong

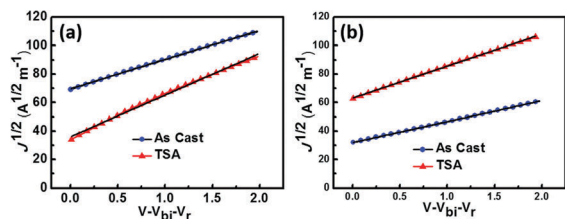


Fig. 5 J - V characteristics for the (a) hole-only and (b) electron-only devices fabricated from DR3TBDD:PC₇₁BM blend films with different treatments.

electron-withdrawing ability as the central core unit was designed and synthesized. After both thermal and solvent vapor annealing, a high PCE of 9.53%, with simultaneously high V_{oc} , J_{sc} and FF values, was achieved. The high V_{oc} value is attributed to the low HOMO energy level of DR3TBDD with an electron-withdrawing BDD central unit, and the high J_{sc} and FF values are attributed to the enhancement of the absorption of blend films, fine-tune morphology and good mobilities. These results indicate that using an electron-withdrawing central unit with a large planar structure in the A-D-A type of small molecules is an efficient way to design high photovoltaic performance small molecules by tuning their HOMO levels.

The authors gratefully acknowledge the financial support from MoST (2014CB643502 and 2016YFA0200200) and NSFC (21404060, 51373078, 51422304 and 91433101).

Notes and references

- B. C. Thompson and J. M. J. Fréchet, *Angew. Chem., Int. Ed.*, 2008, **47**, 58–77.
- Y. J. Cheng, S. H. Yang and C. S. Hsu, *Chem. Rev.*, 2009, **109**, 5868–5923.
- Z. C. He, C. M. Zhong, S. J. Su, M. Xu, H. B. Wu and Y. Cao, *Nat. Photonics*, 2012, **6**, 591–595.
- S. H. Liao, H. J. Jhuo, Y. S. Cheng and S. A. Chen, *Adv. Mater.*, 2013, **25**, 4766–4771.
- J. B. You, L. T. Dou, K. Yoshimura, T. Kato, K. Ohya, T. Moriarty, K. Emery, C. C. Chen, J. Gao, G. Li and Y. Yang, *Nat. Commun.*, 2013, **4**, 1446.
- X. W. Hu, C. Yi, M. Wang, C. H. Hsu, S. J. Liu, K. Zhang, C. M. Zhong, F. Huang, X. Gong and Y. Cao, *Adv. Energy Mater.*, 2014, **4**, 1400378.
- L. Ye, S. Q. Zhang, L. J. Huo, M. J. Zhang and J. H. Hou, *Acc. Chem. Res.*, 2014, **47**, 1595–1603.
- J. D. Chen, C. H. Cui, Y. Q. Li, L. Zhou, Q. D. Ou, C. Li, Y. F. Li and J. X. Tang, *Adv. Mater.*, 2015, **27**, 1035–1041.
- Z. C. He, B. Xiao, F. Liu, H. B. Wu, Y. L. Yang, S. Xiao, C. Wang, T. P. Russell and Y. Cao, *Nat. Photonics*, 2015, **9**, 174–179.
- B. Kan, M. M. Li, Q. Zhang, F. Liu, X. J. Wan, Y. C. Wang, W. Ni, G. K. Long, X. Yang, H. R. Feng, Y. Zuo, M. T. Zhang, F. Huang, Y. Cao, T. P. Russell and Y. S. Chen, *J. Am. Chem. Soc.*, 2015, **137**, 3886–3893.
- S. Zhang, L. Ye, W. Zhao, B. Yang, Q. Wang and J. Hou, *Sci. China: Chem.*, 2015, **58**, 248–256.
- V. Gupta, A. K. K. Kyaw, D. H. Wang, S. Chand, G. C. Bazan and A. J. Heeger, *Sci. Rep.*, 2013, **3**, 1965.
- A. K. K. Kyaw, D. H. Wang, D. Wynands, J. Zhang, T. Q. Nguyen, G. C. Bazan and A. J. Heeger, *Nano Lett.*, 2013, **13**, 3796–3801.
- A. Leliege, C. H. Le Regent, M. Allain, P. Blanchard and J. Roncali, *Chem. Commun.*, 2012, **48**, 8907–8909.
- Y. S. Liu, C. C. Chen, Z. R. Hong, J. Gao, Y. Yang, H. P. Zhou, L. T. Dou, G. Li and Y. Yang, *Sci. Rep.*, 2013, **3**, 1965.
- A. Mishra and P. Bauerle, *Angew. Chem., Int. Ed.*, 2012, **51**, 2020–2067.
- K. Sun, Z. Y. Xiao, S. R. Lu, W. Zajaczkowski, W. Pisula, E. Hanssen, J. M. White, R. M. Williamson, J. Subbiah, J. Y. Ouyang, A. B. Holmes, W. W. H. Wong and D. J. Jones, *Nat. Commun.*, 2015, **6**, 6013.
- Y. M. Sun, G. C. Welch, W. L. Leong, C. J. Takacs, G. C. Bazan and A. J. Heeger, *Nat. Mater.*, 2012, **11**, 44–48.
- T. S. van der Poll, J. A. Love, T. Q. Nguyen and G. C. Bazan, *Adv. Mater.*, 2012, **24**, 3646–3649.
- L. J. Huo, L. Q. Yang, A. C. Stuart, S. C. Price, S. B. Liu and W. You, *Angew. Chem., Int. Ed.*, 2011, **50**, 2995–2998.
- W. Ni, M. M. Li, X. J. Wan, H. R. Feng, B. Kan, Y. Zuo and Y. S. Chen, *RSC Adv.*, 2014, **4**, 31977–31980.
- L. J. Huo, T. Liu, B. B. Fan, Z. Y. Zhao, X. B. Sun, D. H. Wei, M. M. Yu, Y. Q. Liu and Y. M. Sun, *Adv. Mater.*, 2015, **27**, 6969–6975.
- H. R. Feng, M. M. Li, W. Ni, F. Liu, X. J. Wan, B. Kan, Y. C. Wang, Y. M. Zhang, Q. Zhang, Y. Zuo, X. Yang and Y. S. Chen, *J. Mater. Chem. A*, 2015, **3**, 16679–16687.
- L. J. Huo, T. Liu, X. B. Sun, Y. H. Cai, A. J. Heeger and Y. M. Sun, *Adv. Mater.*, 2015, **27**, 2938–2944.
- D. P. Qian, W. Ma, Z. J. Li, X. Guo, S. Q. Zhang, L. Ye, H. Ade, Z. A. Tan and J. H. Hou, *J. Am. Chem. Soc.*, 2013, **135**, 8464–8467.
- D. P. Qian, L. Ye, M. J. Zhang, Y. R. Liang, L. J. Li, Y. Huang, X. Guo, S. Q. Zhang, Z. A. Tan and J. H. Hou, *Macromolecules*, 2012, **45**, 9611–9617.
- M. C. Scharber, D. Mühlbacher, M. Koppe, P. Denk, C. Waldauf, A. J. Heeger and C. J. Brabec, *Adv. Mater.*, 2006, **18**, 789–794.
- B. Walker, C. Kim and T.-Q. Nguyen, *Chem. Mater.*, 2011, **23**, 470–482.
- J. E. Anthony, *Chem. Rev.*, 2006, **106**, 5028–5048.
- A. Guerrero, S. Loser, G. Garcia-Belmonte, C. J. Bruns, J. Smith, H. Miyachi, S. I. Stupp, J. Bisquert and T. J. Marks, *Phys. Chem. Chem. Phys.*, 2013, **15**, 16456–16462.
- Y. Ruiz-Morales, *J. Phys. Chem. A*, 2002, **106**, 11283–11308.
- C.-Z. Li, C.-C. Chueh, H.-L. Yip, K. M. O'Malley, W.-C. Chen and A. K. Y. Jen, *J. Mater. Chem.*, 2012, **22**, 8574–8578.
- S. Miller, G. Fanchini, Y.-Y. Lin, C. Li, C.-W. Chen, W.-F. Su and M. Chhowalla, *J. Mater. Chem.*, 2008, **18**, 306–312.